

MRS Advances © 2017 Materials Research Society. This is an Open Access article, distributed under the terms of the Creative Commons Attribution licence (<http://creativecommons.org/licenses/by/4.0/>), which permits unrestricted re-use, distribution, and reproduction in any medium, provided the original work is properly cited.

DOI: 10.1557/adv.2016.672

Determination of the Forward Dissolution Rate for International Simple Glass in Alkaline Solutions

Alice Elia, Karine Ferrand and Karel Lemmens

SCK•CEN, Belgian Nuclear Research Centre, Boeretang 200 - BE-2400 Mol, Belgium

ABSTRACT

The International Simple Glass (ISG) is considered as reference benchmark glass and is used in the frame of an international collaboration for the study of the dissolution mechanisms of high-level vitrified nuclear waste.

In this work the forward dissolution rate of the ISG was determined in different alkaline solutions, as a simulation of the disposal conditions foreseen by the Belgian concept for geological disposal of vitrified waste. The determination of the forward dissolution rate was done by measuring the Si released from the glass in solution in tests performed at 30 °C in four different KOH solutions with pH varying from 9 to 14 and in artificial cementitious water at pH 13.5.

The forward dissolution rates determined for the ISG in high pH solutions are in good agreement with the results obtained for a lower pH range.

The rates obtained in this study, moreover, were compared with the rates measured in the same conditions for SON68 glass from a previous work. The values obtained for the two glasses are comparable in artificial cementitious water and in KOH at moderately alkaline pH. At higher pH, ISG glass shows a lower forward dissolution rate with respect to SON68 (0.20 g·m⁻²·d for ISG and 0.35 g·m⁻²·d for SON68 at pH 14).

INTRODUCTION

The International Simple Glass (ISG) is used in the frame of a collaboration between six nations studying the dissolution mechanisms of high-level vitrified nuclear waste. Its composition was selected to serve as reference benchmark glass and, for this reason, it is composed of a reduced number of oxides with respect to the more complex SON68 [1,2]. The Belgian concept for geological disposal of vitrified waste foresees a 3 cm thick carbon steel overpack surrounded by a 70 cm thick Ordinary Portland cement buffer. The corrosion of the steel overpack is slowed down by the presence of the cement: indeed, it provides an alkaline environment which passivates the surface of the steel overpack and reduces its corrosion rate. In the long term, perforation of the steel overpack will nevertheless occur, and bring the vitrified waste in contact with the highly alkaline cement pore water, causing release of the radionuclides. To better understand the waste glass dissolution kinetics in these conditions, the dissolution rates for the SON68 and the PAMELA glasses [3] were determined in alkaline media [4]. Similar tests were performed with the ISG.

The behaviour of the ISG was also investigated by different other authors [1,2,5,6], but mainly focussing on its dissolution at near neutral pH, depending on the type of radioactive waste repository chosen by the different countries involved in the collaboration.

EXPERIMENTAL DETAILS

Dynamic tests were performed using 0.8 g of ISG powder with a granulometry range of 125-250 μm . The glass was provided by MoSCI Corporation (Rolla, MO, USA). In order to have homogeneity between samples used by the different research teams, a 50 kg batch of the ISG was produced in May 2012 and glass ingots of 500 g each were then distributed for study [1]. The nominal composition is reported in Table I.

Table I: Nominal ISG composition [1]

Oxide	% w/w
SiO ₂	56.18
B ₂ O ₃	17.34
Na ₂ O	12.17
Al ₂ O ₃	6.06
CaO	4.98
ZrO ₂	3.28

The glass powder was obtained by crushing and grinding a glass ingot. The powder was then sieved and washed in deionized water in an ultrasonic bath and dried in oven at 105°C. The specific surface area was measured by BET (Kr) and is equal to $0.046 \pm 0.002 \text{ m}^2 \cdot \text{g}^{-1}$. The leaching solutions were four different KOH solutions and an artificial cementitious water. The KOH solutions used in this study have a pH of 14.0 ± 0.2 , 13.0 ± 0.2 , 11.5 ± 0.2 and 9.0 ± 0.2 . The artificial cementitious water is here defined as Young Cement Water (YCWCa) and has a pH of 13.5 ± 0.2 . Its composition, determined by ICP-AES and TIC analyses, is given in Table II.

Table II: Composition of the Young Cement Water (pH = 13.5 ± 0.2)

Element	mg·L ⁻¹
Al	<0.2
Ca	26.0 ± 2.6
K	13800 ± 1400
Na	3110 ± 310
Si	1.02 ± 0.14
TIC	5.1 ± 2.2

The experimental setup is shown in figure 1: the glass powder was placed in a PTFE cell with an internal volume of 672 mm³ and the temperature of the oven was set to 30 ± 0.2 °C. The tests were carried out with different flow rates, ranging from $0.06 \text{ ml} \cdot \text{min}^{-1}$ to $0.6 \text{ ml} \cdot \text{min}^{-1}$. In the case of KOH solution at pH 9.0, the Si concentration at the highest flow rate would be too low to be determined by UV-Visible spectrophotometry: for this reason, the flow rates selected for this medium vary from 0.03 to $0.24 \text{ ml} \cdot \text{min}^{-1}$.

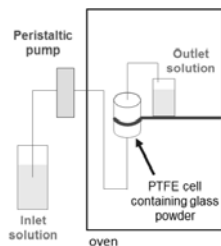


Figure 1: Experimental setup to determine the forward dissolution rate

Samples of the outlet solutions were taken each 30 minutes, for a total duration of around 8 hours. The Si concentration in the samples was measured by UV-Visible spectrophotometry using the blue β -silicomolybdenum method [7]. The concentration measured at the steady-state was used to calculate the glass dissolution rate for each flow rate, according to the equation 1:

$$r = \frac{[Si] \times \left(\frac{F}{S}\right)}{f_i} \quad (1)$$

Where $[Si]$ is the steady-state silicon concentration in the outlet solution ($\text{g}\cdot\text{m}^{-3}$), F is the flow rate ($\text{m}^3\cdot\text{d}^{-1}$), S is the surface area of the glass sample (m^2), f_i is the mass fraction of Si in the glass. The tests were performed in duplicate.

The dissolution rates calculated for each flow rate are then plotted in function of the Si concentration at the steady-state. The uncertainty (two standard deviations) on this dissolution rate is 8%. This value is given by the sum of the uncertainties related to the determination of the Si concentration by UV/Visible spectrophotometry, the determination of the specific surface area of the glass powder and the accuracy of the balance used.

The forward dissolution rate (r_0) is calculated by extrapolation of the regression line to a Si concentration equal to zero (i.e. the intercept of the linear regression). The associated uncertainty, calculated for a 95% confidence interval, is larger than 8%.

RESULTS AND DISCUSSION

The forward dissolution rates determined in the different leaching solutions are presented in Table III. In KOH solutions, we observe a general increase of the forward dissolution rate with the increase of the pH, as previously observed in literature [1,4,8-14] and especially for SON68 glass in similar tests [4].

Figure 2 shows a comparison between the forward dissolution rates obtained for the first series of data obtained for ISG and SON68 in KOH solutions: a good agreement of the results is obtained for moderately alkaline pH values. The duplicate series of experiments gave comparable results, thus is not shown in figure 2. At higher pH values, the r_0 determined for SON68 is slightly higher than the one for the ISG. This discrepancy seems to increase at pH 14, but taking into account the large uncertainty encountered for SON68, the actual difference between the two glasses at this pH is difficult to estimate.

Table III: Forward dissolution rates of ISG glass determined in alkaline media for pH values between 11.5 and 14

Leaching solution	pH	r_0 ($\text{g}\cdot\text{m}^{-2}\cdot\text{d}^{-1}$)	r_0 ($\text{g}\cdot\text{m}^{-2}\cdot\text{d}^{-1}$) duplicate series
KOH	11.5 ± 0.2	$(6.77 \pm 1.78) \times 10^{-2}$	$(6.75 \pm 0.91) \times 10^{-2}$
KOH	13.0 ± 0.2	$(1.12 \pm 0.40) \times 10^{-1}$	$(8.61 \pm 3.37) \times 10^{-2}$
KOH	14.0 ± 0.2	$(2.04 \pm 1.26) \times 10^{-1}$	$(1.75 \pm 0.44) \times 10^{-1}$
YCWCa	13.5 ± 0.2	$(4.12 \pm 3.01) \times 10^{-2}$	$(3.59 \pm 2.02) \times 10^{-2}$

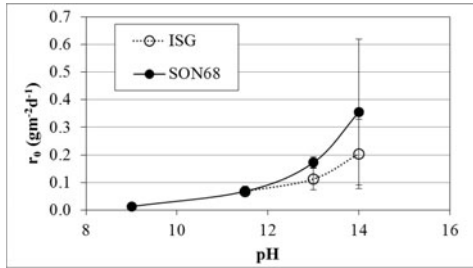


Figure 2: Comparison between r_0 determined in KOH solutions for ISG (1st series) and SON68 as a function of pH

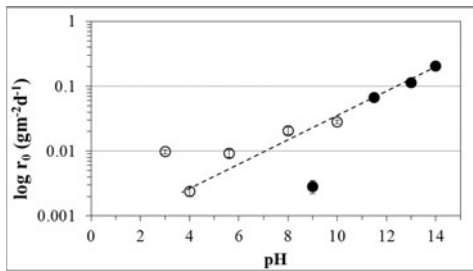


Figure 3: Comparison of r_0 obtained in this study in KOH solutions (full circles) with data reported by Inagaki *et al.* (hollow circles) [5]

The initial dissolution rate of the ISG was determined by Inagaki *et al.* [5] at 25°C in KCl solutions with pH ranging from 3 to 10. As shown in figure 3, the results obtained in our study for the pH range 11.5-14 are in good agreement with their values determined for a lower pH range. The combination of the two data sets confirms the expected increase of the forward dissolution rate with pH.

Table III and figure 3 do not show data obtained with our experimental setup in the pH range tested by Inagaki *et al.* A test was however performed at pH 9 to see if the forward rate would be comparable with the ones found with the microchannel flow-through method [5]. In this test, the ISG did not show the expected behaviour: the dissolution rate, calculated from the dissolved Si

concentration, did not decrease for increasing Si concentrations, as it should do following the first-order rate law [5,12]. On the contrary, the dissolution rate showed a slight increase with increasing Si concentrations. The Si concentrations increased with decreasing flow rate, as expected, but not proportionally. Possibly, at this near-neutral pH, where incongruent dissolution with Si gel formation is favored, the resorption of dissolved Si on the altered glass surface has led to an underestimation of the matrix dissolution rate with respect to the values reported in [5] for pH values between 8 and 10. This would imply that the corresponding rates determined in our setup for the ISG at pH 9 are not forward rates, for which congruent Si dissolution is a prerequisite, especially when Si is used as dissolution indicator. In our setup, with flow rates from 30 to 240 $\mu\text{L}\cdot\text{min}^{-1}$ (at pH 9), and a glass surface area of about 372 cm^2 , the surface normalized flow rate is 0.08 to 0.65 $\mu\text{L}\cdot\text{min}^{-1}\cdot\text{cm}^{-2}$. In the setup used in [5], with flow rates from 2 to 20 $\mu\text{L}\cdot\text{min}^{-1}$, and a glass surface area of about 3 cm^2 , the surface normalized flow rate is 0.67 to 6.7 $\mu\text{L}\cdot\text{min}^{-1}\cdot\text{cm}^{-2}$. Because there is less water renewal per unit of glass surface area in our setup, resorption of Si is more likely. Re-precipitation of Si as a secondary phase is unlikely. The reaction time in the cell for tests at pH 9 is from 1.5 to 12 minutes. For such short reaction time, geochemical modelling results show that the solution was far from saturation with respect to any secondary phase. Precipitation of secondary phases can be ruled out also because silicon concentration is far from saturation with respect to amorphous silica at such high pH. As shown in [5], the dissolution of the ISG is incongruent at lower pH and becomes congruent at pH 10, suggesting that, at higher pH, there is a reduced possibility of having gel formation that could cause resorption of Si. For this reason, the forward rates measured with our setup at pH 11.5–14 are probably not biased by Si resorption. The test with SON68 at pH 9 [4] did not show a clear deviation from the first-order rate law, but it cannot be excluded that the resulting forward rate was also to some extent decreased by Si resorption. It nevertheless fits with the forward rate equation found in [16], so the possible bias is probably small.

Table III also presents the results from the experiments carried out in YCWCa (pH 13.5). In this leaching medium the values of r_0 are lower than the ones obtained in KOH with a similar pH. The lower dissolution rate is due to the presence of calcium in the solution, which can react with the glass surface, increasing in this way its resistance to dissolution [11,17]. The values obtained in YCWCa, moreover, are in good agreement with the forward dissolution rate measured for SON68 glass (unpublished data), which was equal to $4.24 \pm 2.46 \times 10^{-2} \text{ g}\cdot\text{m}^{-2}\cdot\text{d}^{-1}$.

The forward dissolution rate is generally defined as the rate at zero silica concentration. The underlying hypothesis is that the glass surface is in pseudo-equilibrium with H_4SiO_4 in solution. Higher dissolved silica concentrations would increase the protective properties of the gel layer, and thus decrease the dissolution rate. Although our dynamic tests confirm the opposite relation between silica concentrations and dissolution rate at high pH, a consistent interpretation and quantification of the presumed Si saturation concentration is not evident at very high pH. Static tests in YCWCa at 30°C showed a continuous increase of the silica concentrations up to more than 1200 $\text{mg}\cdot\text{L}^{-1}$ for SON68 [18] and even more than 3000 $\text{mg}\cdot\text{L}^{-1}$ for the ISG [19], while the glass was still dissolving. Because the glass dissolution would proceed by a dissolution/precipitation mechanism at this high pH [20], the formed layer would be less protective than a gel layer formed by condensation at near-neutral pH. It could nevertheless constitute a diffusion barrier, leading to a dissolution rate decreasing following the square root of time, as proposed for SON68 in [18]. At more advanced reaction progress, a constant dissolution rate is reached, which would be affinity controlled. The main difference between dissolution at near-neutral and high pH would be that in the former case, the silica concentration affects the

thin Passive Reactive Interface (PRI) between the pristine glass and the gel, whereas at high pH, it would affect the dissolution/precipitation layer. Although the mechanism is thus not identical, the dissolution rate will be maximum at zero silica concentration in both cases.

CONCLUSIONS

The forward dissolution rate of the ISG was determined in different KOH solutions with pH varying from 9 to 14 and in artificial cementitious water at pH 13.5. In comparison to the rates measured previously for SON68 with the same method, the values obtained for ISG are very similar at pH 11.5. At higher pH, instead, the forward dissolution rates of ISG appear to be slightly lower than the ones of SON68, even if the large uncertainties encountered for SON68 make the interpretation more difficult and more tests would be needed to reduce the uncertainty on the forward dissolution rate for SON68 at pH 14. The forward dissolution rates obtained for ISG in the pH range 11.5-14 are nevertheless in good agreement with values reported in literature. This was not the case for the experiments carried out at pH 9, where the values of Si concentration measured in the outlet solution are probably affected by Si resorption in the alteration layer formed on the glass surface, impeding the estimation of the forward dissolution rate. The experiments carried out in artificial cementitious water at pH 13.5 confirmed that, in alkaline solutions, calcium has a positive effect in reducing the forward dissolution rate of glass.

ACKNOWLEDGMENTS

The authors would like to acknowledge the Belgian Agency for Radioactive Waste and Enriched Fissile Materials (NIRAS/ONDRAF) for the financial support.

REFERENCES

1. S. Gin, A. Abdelouas, L. J. Criscenti, W. L. Ebert, K. Ferrand, T. Geisler, M. T. Harrison, Y. Inagaki, S. Mitsui, K. T. Mueller, J. C. Marra, C. G. Pantano, E. M. Pierce, J. V. Ryan, J. M. Schofield, C. I. Steefel and J. D. Vienna, *Mater. Today* **16**, 243-248 (2013).
2. A. Abdelouas, Y. El Mendili, A. Ait Chaou, G. Karakurt, C. Hartnack, J.-F. Bardeau, T. Saito and H. Matsuzaki, *Int. J. Appl. Glass Sci.* **4**, 307-316 (2013).
3. M.I. Ojovan and W.E. Lee, *Metall. Mater. Trans. A* **42**, 837-851 (2011).
4. K. Ferrand and K. Lemmens, *Mater. Res. Soc. Symp. Proc.* **1107**, 287-294 (2008).
5. Y. Inagaki, T. Kikunaga, K. Idemitsu and T. Arima, *Int. J. Appl. Glass Sci.* **4**, 317-327 (2013).
6. M. Fournier, P. Frugier and S. Gin, *Procedia Materials Science* **7**, 202-208 (2014).
7. Q. Zini, P.L. Buldini and L. Morettini, *Microchem. J.* **32**, 148-152 (1985).
8. S.-Y. Jeong and W. L. Ebert, *Mat. Res. Soc. Symp. Proc.* **757**, 159-165 (2002).
9. T. Advocat, J. L. Crovisier, E. Vernaz, G. Ehret and H. Charpentier, *Mat. Res. Soc. Symp. Proc.* **212**, 57-64 (1991).

10. K. G. Knauss, W. L. Bourcier, K. D. McKeegan, C. I. Merzbacher, S. N. Nguyen, F. J. Ryerson, D. K. Smith, H. C. Weed and L. Newton, *Mat. Res. Soc. Symp. Proc.* **176**, 371-382 (1989).
11. C. A. Utton, R. J. Hand, P. A. Bingham, N. C. Hyatt, S. W. Swanton and S. J. Williams, *J. Nucl. Mater.* **435**, 112-122 (2013).
12. R.J. Hand, N.C. Hyatt, S.W. Swanton and S.J. Williams, *J. Nucl. Mater.* **442**, 33-45 (2013).
13. N.J. Cassingham, P.G. Heath, N.C. Hyatt and C.L. Corkhill, *Int. J. Appl. Glass Sci.* **4**, 341-356 (2013).
14. S.W. Swanton, J. Schofield, R.J. Hand, A. Clacher, C.A. Utton and N.C. Hyatt, *Mineral. Mag.* **76**, 2919-2930 (2012).
15. B. Grambow, *Mat. Res. Soc. Symp. Proc.* **506**, 141-152 (1998).
16. P. Frugier, S. Gin, Y. Minet, T. Chave, B. Bonin, N. Godon, J.E. Lartigue, P. Jollivet, A. Ayrat, L. De Windt, and G. Santarini, *J. Nucl. Mater.* **380**, 8-21 (2008).
17. S. Mercado-Depierre, F. Angéli, F. Frizon and S. Gin, *J. Nucl. Mater.* **441**, 402-410 (2013).
18. S. Liu, K. Ferrand, K. Lemmens, *Appl. Geochem.* **61**, 302-311 (2015)
19. K. Ferrand, S. Liu and K. Lemmens, Report No. SCK•CEN-ER-297 (2015)
20. S. Gin, P. Jollivet, M. Fournier, C. Berthon, Z. Wang, A. Mitroshkov, Z. Zhu and J. V. Ryan, *Geochim. Cosmochim. Acta* **151**, 68-85 (2015)